Visualization of Gaseous Fluid Profiles in Solid Electrolyte Dendrites Fabricated by Micro Pattering Stereolithography

Soshu KIRIHARA, Katsuya NORITAKE, Naoki KOMORI and Satoko TASAKI*
*** JWRI, Osaka University 11-1 Mihogaoka, Ibaraki 567-0047, Japan**

KEY WORDS: (Solid Oxide Fuel Cell), (Ceramic Electrolyte Dendrite), (Yttria Stabilized Zirconia), (Micro Pattering Stereolithography), (Finite Element Method), (Computer Aided Design), (Manufacturing and Evaluation)

1. Introduction

Solid oxide fuel cells (SOFCs) are investigated as novel generation systems of electric powers with high efficiencies in energy conversion circulations. Yttria stabilized zirconia (YSZ) with high ion conductivities for incident oxygen is widely adopted material for solid electrolyte anodes as the SOFC components [1-5]. Recently, porous network structures were introduced into YSZ electrodes in micrometer or nanometer sizes to increase surface areas of reaction interfaces and gap volumes of stream paths [6-8]. In this investigation, solid electrolyte dendrites composed of YSZ spatial lattice structures with various coordination numbers were fabricated successfully by using micro pattering stereolithography and powder sintering techniques. In the dendrite structure, stress distributions and fluid flows were simulated and visualized by using finite element methods. These new computer aided designs, manufactures and evaluations have been established and optimized to create micro components of various ceramics in our investigation group [9-17].

2. Experimental Procedures

The solid electrolyte dendrites with spatial lattice structures were designed by using a computer graphic application (Think Design: Toyota Caelum, Japan) as shown in Fig. 1. These surface areas of reaction interfaces and the gap volume of stream paths were calculated geometrically for the dendrite lattice with four coordination numbers as shown in Fig. 2. The dendrite lattices of 1.16 in aspect ratio can be considered to exhibit the higher reaction efficiencies and gas transmittances according to Nernst equation. In the optimized dendrite structure, the diameter and length of YSZ rods were decided 92 and 107 μm, respectively. The lattice constant was 250μm. The graphic data was converted into a stereolithographic format through polyhedral approximations. The solid model was sliced into the cross sectional numerical data sets to input the stereolithographic equipment (D-MEC: SI-C1000, Japan,). Photo sensitive acrylic resin dispersed with YSZ particles of 60 and 100 nm in first and second diameters at 30 volume % were fed over a substrate from a dispenser nozzle. The highly viscous resin paste was fed with controlled air pressure, and spread uniformly by a mechanical knife edge. The thickness of each layer was controlled to 10 μm. The cross sectional pattern was formed through illuminating visible laser of 405 nm in wavelength on the resin surface. The high resolution image could be achieved by applying a digital micro mirror device (DMD) and an objective optical lens. Figure 3 shows a schematic illustration of the micro patterning stereo- lithography system. The DMD is an optical element assembled by micro mirrors of 14 μm in edge length. The tilting of each tiny mirror can be controlled according to the cross sectional data transferred form a computer. The solid micro structures were built by stacking these patterns layer by layer. In order to avoid deformation and cracking during dewaxing, careful investigation for the heat treatment processes were required. The formed precursors with dendrite structures were heated at various temperatures from 100 to 600 °C while the heating rate was 1.0 °C /min. The dewaxing process was observed in respect to the weight and color changes. The YSZ particles could be sintered at 1500 °C for 2 hs. The heating rate was 8.0 °C/min. The density of the sintered sample was measured by using Archimedes method. The ceramic microstructures were observed by a digital optical microscope and scanning electron microscopy. In the lattice dendrites, fluid flow velocities and pressure stress distributions were simulated and visualized by a finite volume method (FVM) application (Ansys: Cybernet Systems, Japan).

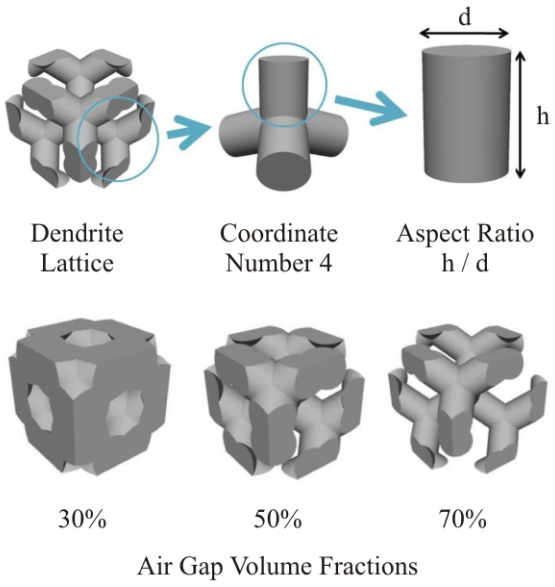

Fig. 1 Computer graphic models of lattice distributions in dendrite structures with coordination number four. Air gap volume fractions are changed continuously according to variation of aspect ratios of the dendrite lattice.

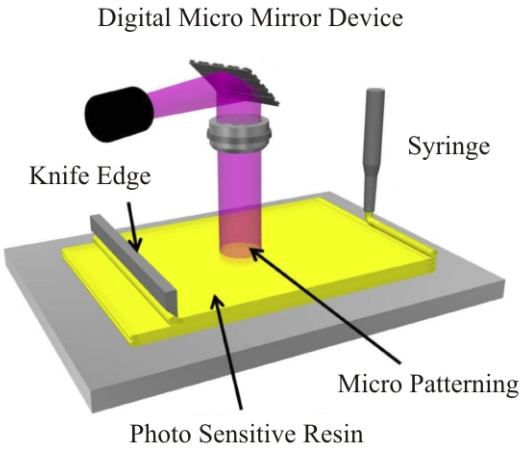

Fig. 2 A schematic illustration of micro patterning stereolithography. Fine images are exposed by using a digital micro mirror device on a photo sensitive resin.

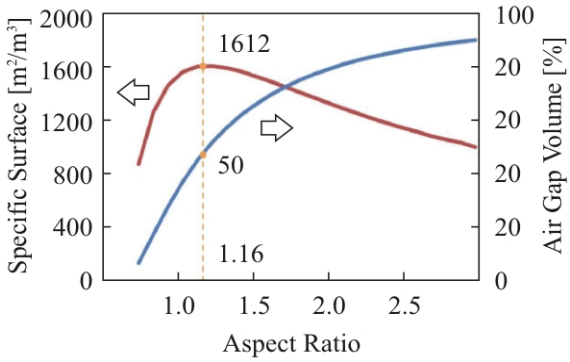

Fig. 3 Optimization of the aspect ratio to obtain the widest specific surface and higher air gap volume. The aspect ratio was decided as 1.16 for designing.

3. Results and Discussion

The dendrite lattice structures composed of the YSZ dispersed acrylic resins were processed exactly by using the stereolithography as shown in Figure 4. The spatial resolution was approximately 1.0 %. The microstructure of the composite lattice is shown in Figure 5. The nanometer sized YSZ particles were dispersed homogeneously in the acryl matrix. Figure 6 shows the sintered solid electrolyte dendrite with the YSZ micro lattice structure. The deformation and cracking were not observed. The linear shrinkages on the both horizontal and vertical axis were 32 %. The volume fraction of the air gaps was 50 % by the open paths. In the other previous investigations, the porous electrodes were formed by sintering the YSZ surly with polystyrene particles dispersion. Therefore, it is difficult to realize the prefect opened pores structures with the higher porosity over 40 % in volume fraction. Figure 7 shows the dense microstructure of the YSZ lattice. The average grain size was approximately 4 μm. The relative density reached at

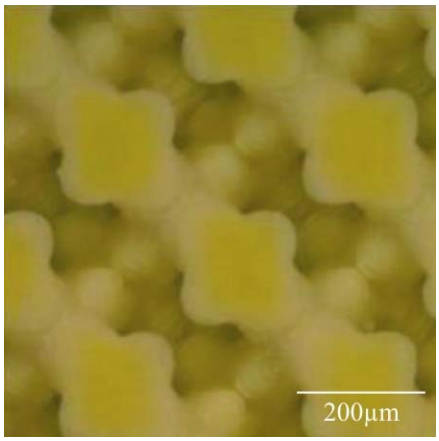

Fig. 4 Acryl dendrite lattice with YSZ particles dispersion fabricated by using the stereolithography.

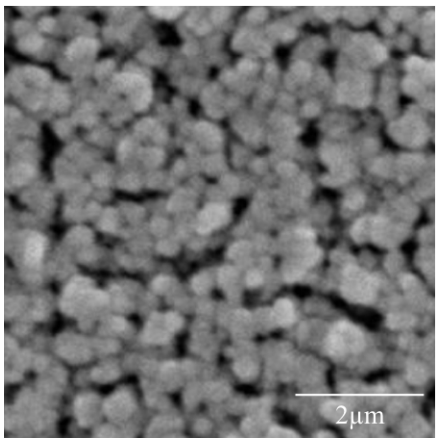

Fig. 5 The nanometer sized YSZ particles in the acryl dendrite lattice. The volume fraction is 30 %.

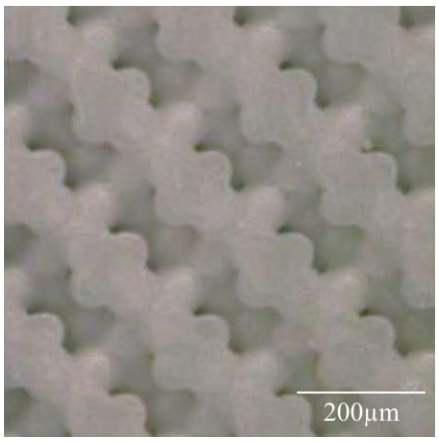

Fig. 6 The sintered dendrite lattices of YSZ solid electrolyte. The part accuracy of the lattice is 2 μm.

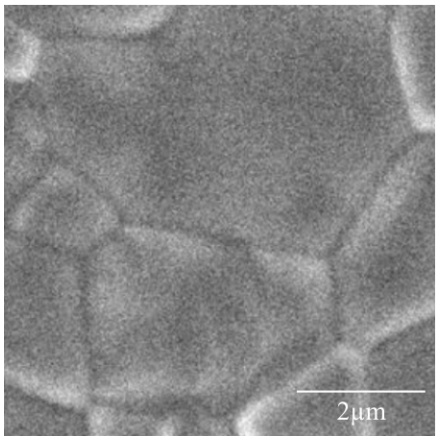

Fig. 7 The microstructure of YSZ micro lattice in the dendrite structure. The average grain size is 4μm.

95 %. Micrometer sized cracks or pores were not observed. The obtained dense YSZ lattice structure will be exhibit the higher performances in mechanical properties as the porous electrodes of the solid electrolyte dendrites. The fluid flow velocities were visualized by using the FVM method as shown in Figure 8. Continuously curved lines indicate the fluid distributions along the vector directions of flow velocities. All air paths were opened for outsides and connected with each others in the YSZ dendrite lattice structures. The fluid flows can transmit the one direction smoothly. The pressure stress distributions in the dendrite were visualized as shown in Figure 9. The fluid pressures were gradually distributed for flow direction, and the localization of the stress was not observed. The fabricated solid electrolyte dendrites with YSZ lattice structures can be considered to have higher performances as novel ceramic electrodes in near future SOFCs.

Conclusion

We have fabricated solid electrolyte dendrites with yttria stabilized zirconia lattices for anode electrodes of solid oxide fuel cells. Acryl precursors including ceramic particles were formed successfully by using micro patterning stereolithography of computer aided design and manufacturing. Thorough careful optimization of process parameters in dewaxing and sintering, we have succeeded in fabricating dense ceramic micro components. These solid electrolyte dendrites with opened air path networks exhibited effective transmission properties of fluid flows. These novel ceramic electrodes have potentials to contribute for developments of compact fuel cells.

Acknowledgments

This study was supported by Priority Assistance for the Formation of Worldwide Renowned Centers of Research - The Global COE Program (Project: Center of Excellence for Advanced Structural and Functional Materials Design) from the Ministry of Education, Culture, Sports, Science and Technology (MEXT), Japan.

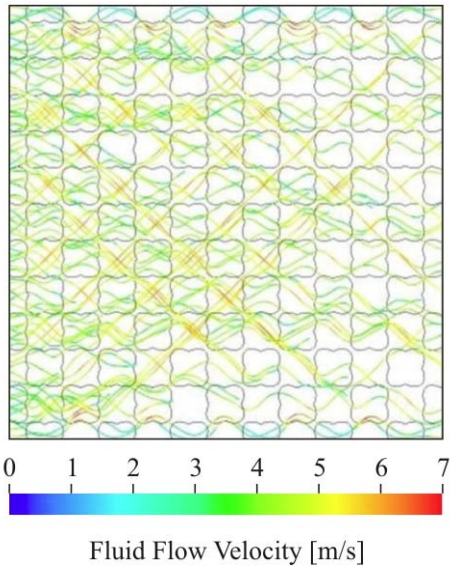

Fig. 8 A distribution of fluid flow velocities in the dendrite lattice structure simulated and visualized by using a FVM method. The curved lines show the fluid flow paths according to the velocity vectors.

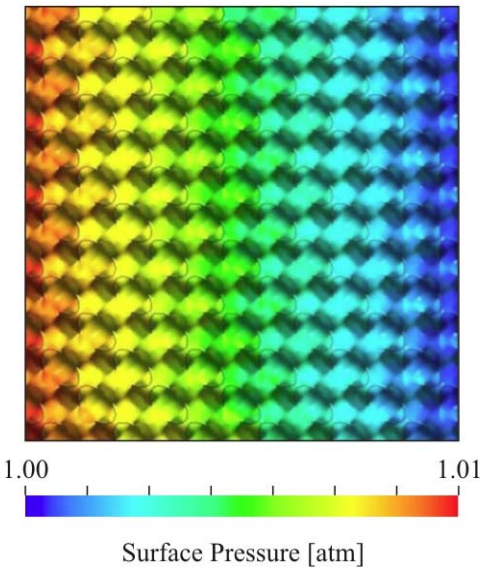

Fig. 9 The distribution of the surface pressure on the ceramics lattice of dendrite structure. The red and blue areas show the higher and lower gas pressures on the reaction interfaces, respectively.

References

[1] N. Minh, Journal of the American Ceramic Society, 76 (1993) 563-588.
[2] S. Singhal, Solid State Ionics, 152 (2002) 405-410.
[3] A. Stambouli, E. Traversa, Renewable Sustainable Energy Reviews, 6 (2002) 433–455.

[4] T. Ramanarayanan, S. Singhal, E. Wachsman, The Electrochemical Society Interface, 10 (2001) 22-27.
[5] J. Will, A. Mitterdorfer, C. Kleinlogel, D. Perednis, L. Gauckler, Solid State Ionics, 131 (2000) 79-96.
[6] J. Hua, Z. Lüa, K. Chena, X. Huanga, N. Aia, X. Dub, C. Fub, J. Wanga, W. Su, Journal of Membrane Science, 318 (2008) 445-451.
[7] J. Haslam, A. Pham, B. Chung, J. Dicarlo, R. Glass, Journal of American Ceramic Society, 88 (2005) 513-518.
[8] T. Talebi, M. H. Sarrafi, M. Haji, B. Raissi, A. Maghsoudipour, International Journal of Hydrogen Energy, 35 (2010) 9440-9447.
[9] W. Chen, S. Kirihara, Y. Miyamoto, Joiurnal of the American Ceramic Society, 90 (2007) 2078-2081.
[10] W. Chen, S. Kirihara, Y. Miyamoto, Applied Physics Letter, 91 (2007) 153507-1-3.
[11] W. Chen, S. Kirihara, Y. Miyamoto, Journal of the American Ceramic Society, 90 (2007) 92-96.
[12] W. Chen, S. Kirihara, Y. Miyamoto, Applied Physics Letters, 92 (2008) 183504-1-3.
[13] H. Kanaoka, S. Kirihara, Y. Miyamoto, Journal of Materials Research, 23(2008) 1036-1041.
[14] Y. Miyamoto, H. Kanaoka, S. Kirihara, Journal of Applied Physics, 103 (2008) 103106-1-5.
[15] S. Kirihara, Y. Miyamoto, K. Takenaga, M. Takeda, K. Kajiyama, Solid State Communications, 121 (2002) 435-439.
[16] S. Kirihara, M. Takeda, K. Sakoda, Y. Miyamoto, Solid State Communications, 124 (2002) 135-139.
[17] S. Kirihara, Y. Miyamoto, The International Journal of Applied Ceramic Technology, 6 (2009) 41-44.
[18] S. Kirihara, T. Niki, M. Kaneko, Journal of Physics, 65 (2009) 12082-1-6.
[19] S. Kirihara, T. Niki, M. Kaneko, Ferroelectrics, 387 (2009) 102-11.
[20] S. Kirihara, K. Tsutsumi, Y. Miyamoto, Science of Advanced Materials, 1 (2009) 175-81.